FAR INFRARED DETECTOR ARRAYS FOR A SOFIA ECHELLE SPECTROMETER

E. F. Erickson, M. R. Haas, J. A. Baltz, S. W. J. Colgan, D. H. Lynch, M. E. McKelvey, and J. Wolf †

NASA-Ames Research Center, MS 245-6, Moffett Field, CA 94035-1000
† DLR Institut für Weltraumsensorik, Rudower Chausee 5, D-12489 Berlin
email: erickson@cygnus.arc.nasa.gov, haas@cygnus.arc.nasa.gov, baltz@cygnus.arc.nasa.gov, colgan@cygnus.arc.nasa.gov, lynch@eestools.arc.nasa.gov, mmckelvey@mail.arc.nasa.gov, Juergen.Wolf@dlr.de

Abstract

Technologies being examined for far-infrared two-dimensional discrete germanium detector arrays are described. We consider both cryogenic readouts and light collector/integrating cavity designs.

1. INTRODUCTION

An Airborne Infrared Echelle Spectrometer (AIRES) (Haas *et al.* 1996) for SOFIA (Erickson and Davidson 1995) is under study as an extension of the concept for the Cryogenic Grating Spectrometer (CGS, Erickson *et al.* 1995), which was operated on the Kuiper Airborne Observatory (KAO) for over a decade. Like the CGS, AIRES would cover the spectral range from 16-210 μm. Unlike the CGS, AIRES will use two-dimensional detector arrays to operate as a long slit spectrograph. Some of the detector technology discussed here for AIRES should be applicable to other FIR instruments as well.

2. DETECTOR CONSIDERATIONS

Based on currently available and anticipated technologies, the 16–210 μm wavelength range can be effectively spanned with three detector types as shown in Figure 1. For the 16–40 μm range, we would use a commercially available Si:Sb Impurity Band Conductor (IBC) array (75 μm pixels, 128 x 128 format). As in the CGS, instead of the traditional Ge:Ga photoconductors (PCs), we plan to use Ge:Sb PCs to cover the 40–125 μm range because their longer wavelength cutoff (Beeman *et al.* 1996) provides better sensitivity for the astrophysically interesting CO(118, 124 μm), HD(112 μm), and [N II](122 μm) lines. We consider stressed Ge:Ga PCs to be the best candidate for the 125–210 μm range. Bolometers were not considered, despite continuous progress in that technology, because they do not readily accommodate the range of backgrounds anticipated, and require special refrigeration. Likewise the Ge IBCs (Watson *et al.* 1993) still suffer from low quantum efficiencies, although they may eventually improve upon the performance of stressed Ge:Ga detectors.

The pitches selected for the three arrays would provide diffraction-limited ($1.2\lambda/D$) pixels at 20, 80, and 160 μm, respectively. This corresponds to pitches of 0.5, 2, and 4 mm for a plate scale $\sim$ 4 arcsec/mm. The array formats described in Table 1 would provide a $\sim$3 arcmin long slit on the sky and a velocity bandwidth $\sim$ 200–550 km/s for a single grating position; these parameters are established by the nature of the sources we expect to study. In addition to AIRES' significant mapping capability, its increase in spectral resolution over that of the CGS provides more dynamical information about the observed gas, larger line-to-continuum ratios for unresolved lines, and higher sensitivity due to the reduced background on the detectors. Table 1 shows the estimated parameters and performance of AIRES on SOFIA for observations of some key astrophysical lines. The large number of pixels will require multiplexed readouts. The requirements for these readouts can be determined from the expected detector backgrounds and integration times.

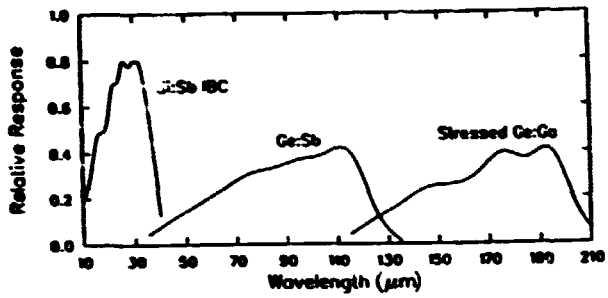

Figure 1: Nominal relative response of the proposed AIRES detector types versus wavelength.

3. CRYOGENIC READOUTS FOR DISCRETE GERMANIUM PHOTOCONDUCTORS

Limited testing of existing cold multiplexers suggests the Hughes SBRC 1 x 32, DC-coupled CRC-696 CTIA developed for SIRTF (Young 1994) can be extended to satisfy requirements for AIRES. Relative to the SIRTF application, ours requires accommodating (1) larger backgrounds, (2) a wider range of backgrounds, (3) the need to synchronize sampling with chopping, and (4) the need to sample faster because of chopping. These factors lead to a consider-

able range of parameters even for a single instrument. Happily item (4) tends to mitigate the demands of item (1).

Table 2 summarizes detector expectations and readout requirements for the AIRES germanium arrays. The expected detector parameters (temperature, bias, responsivity, and dark current) are based on our KAO experience for optimized operation of both types of Ge detector. The minimum and maximum "Operating Range" fluxes and photocurrents were calculated based on the expected operation of AIRES. The requirement to chop the signal to suppress sky noise restricts the maximum contiguous value of the integration time to be $10 \lesssim t \lesssim 50$ ms, corresponding to chopping from ~8–35 Hz, allowing for chopper rise times. To allow for uncertainties, the "AIRES Requirements" for read noise are based on half the estimated minimum flux, and those for well capacity are based on twice the estimated maximum flux. Clearly a good understanding of the instrument and detectors is essential to specify the readouts.

The table also shows the CRC-696 CTIA performance for comparison with the requirements. The device is inadequate in several parameters, but the technology is promising because of its low operating temperature, low power dissipation, low read noise, and compatibility with efficient sampling techniques (Fowler & Gatley 1993). Read noises corresponding to the two maximum well capacities w are 10^5 times smaller than w, permitting 1% measurements over an assumed dynamic range of 1000 for the device. Also, the maximum well capacity requirement can be reduced by sampling faster, subject to retaining the other parameters within range. For example, faster sampling increases power dissipation in the device and increases the read (amplifier and switching) noise, but according to Hughes this multiplexer should operate at much higher frequencies than the 30 Hz used in our tests.

Principal concepts to be explored in extending the CRC-696 technology are (1) larger feedback capacitors on chip to boost the well capacity, (2) external selection of feedback capacitors to accommodate the range of backgrounds, (3) significantly higher clock rates appropriate for use with a chopper, (4) higher input offset stability, (5) lower input capacitance (and whether it is a significant benefit), (6) improved input offset uniformity, (7) reduced debiasing at the input as the wells fill, and (8) the possibility of auto-zero circuitry (AC-coupling the input). All of these issues have ramifications. For example, a larger feedback capacitor reduces the gain (volts out per electron in), requiring increased external gain and band limiting. We note that the stressed detectors' requirements in Table 2 are further from the performance achieved by the CRC-696 than are those for the unstressed detectors, so suitable readouts may take longer to develop.

4. Ge:Sb DETECTOR ARRAY

Material Development: We have sponsored development of new Ge:Sb detector material for our unstressed arrays at LBL (Beeman *et al.* 1996). The advantage of Ge:Sb over the well-characterized Ge:Ga is its longer wavelength coverage. Our experience with this material in the CGS was satisfactory, even though optimum performance required individual bias voltages and polarities for each detector. This flexibility is not possible with the cryogenic multiplexers planned for AIRES. Beeman *et al.* (1996) report the new material does not have these nonuniformities and is effectively equivalent in sensitivity, responsivity, and dark current to the best available Ge:Ga material. Maximum sensitivity for our backgrounds is achieved at ~3.0 K and 200 mV bias, very consistent with our CGS experience.

Bare vs. Cavity-Mounted Detectors: The quantum efficiency of bulk germanium detectors is a concern. The absorption length which is large compared to the desired detector size, and the high index of refraction which produces efficient reflection of incident light, both suggest the use of integrating cavities to increase the quantum efficiency.

Measurements of light collection efficiency – or the responsivity ηG – are difficult. The recent measurements at LBL of both our new Ge:Sb material and high quality Ge:Ga material gave responsivities ~3 A/W at 90 μm for maximum sensitivity (bias and temperature) conditions. These measurements were made with the chips in standard LBL cavities. This responsivity corresponds to $\eta G \simeq 0.04$, and at these relatively low biases, $G \simeq 1$. Under quite similar conditions for Ge:Sb detectors in the CGS cavities our responsivity was $\gtrsim$10 A/W or $\eta G \gtrsim 0.1$. Wang *et al.* (1986) found that bare detector chips with a special geometry had ηG values approaching those for chips in cavities, although the best cavity-mounted detector had 60% higher responsivity than the best bare detector. These tests did not employ light concentrators, which should improve the performance of cavities.

Light Collector/Integrating Cavity Optical Analysis: Our detector light collector/integrating cavity designs have been guided by ray-trace evaluations using *Opticad* and *ASAP*. The latter program treats polarization effects and is better able to handle realistic cavity designs imported from our design software *Pro/ENGINEER*. Calculations indicate that the cavity efficiency is generally high

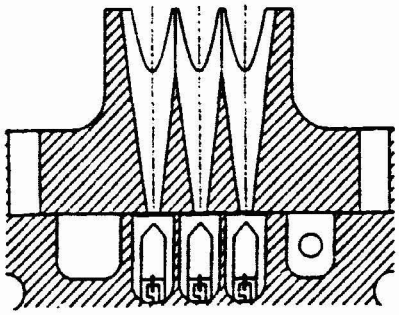

Figure 2: Cross-section of the prototype Ge:Sb detector array geometry.

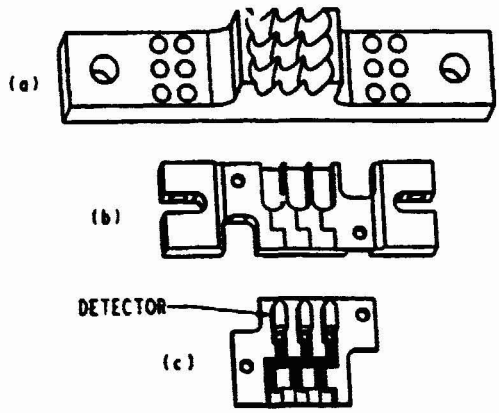

Figure 3: Isometric views of prototype array parts.

(≳85%), but that improvements in light absorption efficiency can be obtained by optimizing the light collector cone height, exit aperture diameter, and detector shape and location in the cavity. Diffraction losses should be small because the cone exit aperture is ~4× the longest wavelength (*i.e.*, multimode operation). The single mode cone/cavity designs used at sub-mm wavelengths are inappropriate because of the large wavelength range covered by our arrays.

Prototype 2-D Ge:Sb Array: We have built a 3×3 Ge:Sb prototype detector array with conical light collectors and integrating cavities on a 2-mm pitch. Figure 2 depicts the concept in cross-section. The design (Figure 3) combines a cone assembly (a) and cavity blocks (b) machined from molybdenum with alumina (polycrystalline sapphire) wafers (c) holding the detectors and leads. These two materials have nearly identical thermal contraction between room and cryogenic temperatures. Wire electrical discharge machining (EDM) of the cones yields a peak-to-peak surface roughness of approximately ~4 μm, nominally adequate for our wavelengths; polishing should significantly reduce this roughness. The computerized EDM process permits optimization of cone geometry, as long as the sides are straight. Each detector has one face conductive-epoxied to a gold-plated surface on the alumina substrate, which serves as the "floor" of the cavity, and the other lead is wire-bonded to a signal trace on the alumina substrate (Figure 3).

Plans: We will optimize the prototype design using Ge:Sb detectors and transimpedence amplifiers in the CGS, and then compare its performance with bare detectors to quantitatively determine the merits of this approach. Assuming our test results validate the design, we would extend the prototype concept to larger formats and possibly a smaller pitch. For example, a 16 × 24-pixel array would be assembled from four 4 × 24 modules. Each row of a module would consist of 24 Ge:Sb chips mounted on an alumina substrate holding the cryogenic multiplexer and mated to a molybdenum cavity block – basically as depicted for parts (b) and (c) Figure 3. Four rows of detectors would be bolted to a 4 × 24 light collector cone block supported by a "U"-bracket with an printed circuit "fan-in" wafer to complete the module.

Our 8 × 12-element array of stressed detectors would incorporate as much of the technology currently under development for the Ge:Sb array and for FIRST (Wolf *et al.* 1996) as possible. As already discussed, the multiplexer development will support both Ge arrays, as would the warm drive and readout electronics.

5. REFERENCES

Beeman, J., Haller, E., & Hanson, W. L. 1996, this volume

Erickson, E. F., Haas, M. R., Colgan, S. W. J., Simpson, J. P., & Rubin, R. H. 1995, in ASP Conf. Series, Vol. 73, "Airborne Astronomy Symposium on the Galactic Ecosystem: From Gas to Stars to Dust," ed. M. R. Haas, J. A. Davidson, & E. F. Erickson (San Francisco, ASP), 523

Erickson, E. F. & Davidson, J. A., in ASP Conf. Series, Vol. 73, "Airborne Astronomy Symposium on the Galactic Ecosystem: From Gas to Stars to Dust," ed. M. R. Haas, J. A. Davidson, & E. F. Erickson (San Francisco, ASP), 707

Haas, M. R., Erickson, E. F., Baltz, J. A., Colgan, S. W. J., Lynch, D. H., & Sablan, M. 1996, this volume

Fowler, A. M., & Gatley, I. 1993, NOAO Preprint No. 386

Wolf, J., Katterloher, R., Lemke, D., Grožinger, U., Hermans, L., Frenzel, O., Engemann, D., Beeman, J., & Fabbricotti, M. 1996, this volume

Young, E. T. 1994, ProcSPIE, 2226, 21

Table 1: AIRES' Parameters and Performance for Representative Wavelengths

Detector Type	Pixel Spacing (μm)	Format (Spectral x Spatial)	λ (μm)	$\frac{1.2\lambda}{D_{SOFIA}}$ (")	Slit Width (")	Echelle Order	Spectral Resol. ($\lambda/\delta\lambda$)	Velocity Resol. (km/s)	Total Bandwidth (km/s)	System NEP[a]	MDLF[b] (1 Hr, 4σ)	Detector Background[c]
Si:Sb IBC	75	128 x 128	18.7	1.9	2	67	60900	4.9	470	12	16	4
			25.2	2.5	4	50	44500	6.7	440	10	14	3
			33.5	3.3	4	37	32100	9.3	530	6	8	4
			36.0	3.6	4	35	37300	8.0	440	6	8	4
Ge:Sb PC	2000	12 x 26	51.6	5.1	8	24	16100	19	190	66	92	86
			63.2	6.3	8	20	18500	16	160	25	35	77
			88.4	8.8	12	14	10800	28	200	12	17	85
			112	11.1	12	11	9300	32	210	11	15	26
Ge:Ga PC (Stressed)	4000	6 x 13	145	14.4	16	8	4500	66	300	21	29	148
			158	15.6	20	8	7600	39	160	19	14	111
			205	20.3	24	6	4800	62	210	20	28	54

[a] Units are 10^{-16} W/$\sqrt{\text{Hz}}$ [b] Minimum Detectable Line Flux, units are 10^{-22} W/cm^2 [c] Units are 10^6 photon/s

Table 2: Cryogenic Readout Considerations for AIRES

Representative Detector Parameters				
Material	stressed Ge:Ga		Ge:Sb	
Wavelength (μm)	180		90	
Bias (mV)	20		200	
Temperature (K)	1.9		2.8	
Capacitance with leads (pF)	0.4		0.7	
Responsivity ηG	0.1		0.1	
Dark Current (e^-/s)	$1x10^4$		$1x10^5$	
Integration time t (ms)	10 - 50		10 - 50	
Dark charge (e^-)	100 - 500		1000 - 5000	
Operating Range:	Minimum	Maximum	Minimum	Maximum
Incident flux (photons/s)†	$5x10^7$	$2x10^9$	$2x10^7$	$3x10^9$
Photocurrent (e^-/s)	$5x10^6$	$2x10^8$	$2x10^6$	$3x10^8$
Photo charge (e^-)	$5 - 25x10^4$	$2 - 10x10^6$	$2 - 10x10^4$	$3 - 15x10^6$

Readout Characteristics					
Quantity	AIRES Requirements				CRC 696°
Well capacity [for t=50 ms] (e^-)	$5x10^5$	$2x10^7$	$2x10^{5}$°	$3x10^7$	$3x10^5$
Read noise (e^-)	110°,‡	200°,τ	50°,‡	300°,τ	30
Input capacitance (pF)	0.4		0.7		1.5
Input node stability (mV)	<0.1		<1		<2
Input offset uniformity (mV)	<1		< 10°		4‖
Input debiasing for full well (mV)	<2		< 20°		<5
Full frame sample rate (Hz)	500 - $1x10^{5}$*				4
Gain uniformity	± 10%°				± 10%
Temperature (K)	1.5-3.5°				1.5
Total power dissipation (μW)	$\lesssim$1000°				32
Format	1x32 linear°				←
Outputs	1°				←
Addressing	random access with 5 address lines°				←
Readout mode	non-destructive, multiple sampling°				←
Reset	global°				←

† Flux range includes effects of changing wavelength, spectral resolution, transmission, aperture, and source.
° Values are nominal CRC 696 performance according to the manufacturer.
* Indicates compatibility with nominal CRC-696 performance.
‡ For t=10 msec.
τ Permits dynamic range of 1000 with maximum statistical error of 1%.
‖ Requires hand selection of parts because of low yields.